Ultrasonics Sonochemistry 81 (2021) 105862

Contents lists available at ScienceDirect

Ultrasonics Sonochemistry

journal homepage: www.elsevier.com/locate/ultson

Bacteriostatic effects of high-intensity ultrasonic treatment on *Bacillus subtilis* vegetative cells

Wei Luo [a,1], Jinqiu Wang [a,1], Yi Wang [a], Jie Tang [a], Yuanhang Ren [b], Fang Geng [a,*]

[a] Institute for Egg Science and Technology, School of Food and Biological Engineering, Chengdu University, No. 2025 Chengluo Avenue, Chengdu 610106, China
[b] Key Laboratory of Coarse Cereal Processing (Ministry of Agriculture and Rural Affairs), Sichuan Engineering & Technology Research Center of Coarse Cereal Industrialization, School of Food and Biological Engineering, Chengdu University, No. 2025 Chengluo Avenue, Chengdu 610106, China

ARTICLE INFO

Keywords:
Ultrasound
Bacillus subtilis
Proteomic analysis
ABC transporter
Two-component system
TCA cycle

ABSTRACT

The bacteriostatic effects of high-intensity ultrasonic treatment (HIU) on *Bacillus subtilis* vegetative cells were evaluated, and the related mechanisms were explored using quantitative proteomics. The bacteriostatic effect of HIU on *B. subtilis* was proportional to the ultrasound treatment time and power, and the number of cultivable *B. subtilis* cells was decreased by approximately one log (at 270 W for 15 min) or half log (at 90 W for 25 min or 360 W for 5 min). Scanning electron microscopy images and gel electrophoresis results showed that HIU caused the destruction of the cell structure and intracellular protein leakage. In addition, HIU treatment at 270 W for 15 min resulted in the greatest decrease (84.22%) in intracellular adenosine triphosphate (ATP) content. The quantitative proteomic analysis showed that *B. subtilis* resisted the stress of HIU treatment by regulating the key proteins in physiological activities related to membrane transport (ATP-binding cassette [ABC] transporter), signal transduction (the two-component system), and energy metabolism (the tricarboxylic acid [TCA] cycle). HIU-induced physical damage, stress, and metabolic disorders were the main causes of the bacteriostatic effects on *B. subtilis*. These findings provide a foundation for the subsequent optimization and potential applications of HIU inactivation of *B. subtilis*.

1. Introduction

Spore-producing bacteria are a major obstacle to decontamination processes in the food industry as they can form highly resistant budding spores in extreme environments, allowing them to survive conventional sterilization methods such as thermal pasteurization[1–3]. Moreover, under suitable conditions, the surviving spore-producing bacteria can quickly resume normal growth and proliferation, thereby posing a great risk to food quality and safety[4–6]. In the food industry, treatments such as high-temperature heating are often used for effective control of spore-producing bacteria[7]. However, heat treatment often has negative effects on the nutritional and organoleptic qualities of food[8]. In addition, to meet the rapid pace of modern lifestyles, the demand for ready-to-eat, fresh, and healthy food has continued to increase, bringing new challenges associated with the control of spore-producing bacteria [9]. The need for safer, efficient, and energy-saving alternative sterilization methods has driven research into new sterilization technologies.

Ultrasonic sterilization technology uses ultrasound to induce vibration cavitation, and then sonoporation, sonochemistry, sonoluminescence, or other methods to kill or inhibit microorganisms on a very fast timescale[10]. In recent years, ultrasound has emerged a key research topic in food engineering technology because of its effective antibacterial properties, and its use has been widely adopted in the food processing industry. For example, excellent (68.91%) inhibition of *Escherichia coli O157:H7* was achieved with ultrasonic treatment of 100 W for 7 min and a power density of 50 W/cm^2, whereas another study proposed a mechanism of action in which free radicals generated by acoustic cavitation entered *E. coli O157:H7* through activated mechanosensitive channels, leading to an increase in intracellular reactive oxygen species levels, and, consequently, cell death[8,11]. Different ultrasound conditions led to log 1.0–8.7 decreases in *Salmonella* species in different food matrices[12]. However, there have been relatively few investigations into the mechanism and effects of ultrasound on spore-producing bacteria. Some preliminary studies have been performed, including a report that ultrasound treatment at 120–480 W for 30 min reduced *Alicyclobacillus acidoterrestris* spores by approximately 1 log,

* Corresponding author.
E-mail address: gengfang@cdu.edu.cn (F. Geng).
[1] These authors contributed equally to this work.

https://doi.org/10.1016/j.ultsonch.2021.105862
Received 29 October 2021; Received in revised form 25 November 2021; Accepted 6 December 2021
Available online 7 December 2021

and that ultrasound treatment at 5000 W and 80% amplitude for 10 min inactivated nutrient cells of *Anoxybacillus flavithermus* and *Bacillus coagulans* in skim milk by 4.26 and 4.53 log, respectively. However, further studies are needed to determine the optimal treatment conditions and the corresponding mechanisms of inhibition[13,14].

Therefore, the aims of this study were to investigate the inhibitory effect of ultrasound on *Bacillus subtilis* and to examine the inhibitory mechanisms using label-free quantitative proteomics. These results will allow further exploration of the specific effectiveness and potential use of ultrasound against *B. subtilis*, as well as provide a theoretical basis for the use of ultrasound sterilization technology in the food industry and methodological guidance for expanding its applications.

2. Materials and methods

2.1. Bacillus subtilis

The strain was obtained by isolation and purification in a laboratory environment and was identified as *B. subtilis* (CP010052.1). As described previously[9], the screened individual colonies were incubated in 20 mL of nutrient broth medium (NB, Haibo Biotechnology Co., Ltd., Qingdao, China) at 37 °C for 12 h in a 150 rpm thermostatic culture shaker (Model ZWY-1102C, Zhicheng Instrument Manufacturing Co., Ltd., Shanghai, China). The cultured suspensions were transferred to nutrient agar medium (NA, Haibo Biotechnology Co., Ltd., Qingdao, China) plates, incubated for 24 h at 37 °C and stored at 4 ℃. A single colony in NA medium was picked, transferred to 20 mL NB medium, mixed well, and incubated at 37 ℃ for 11 h with shaking at 150 rpm. Then, the culture solution was aspirated, 1% culture solution was added to 20 mL fresh NB, and the plates were incubated for 11 h under the same conditions described above to obtain the initial stable growth of the bacterial solution. To generate a working solution, 2 mL of bacterial solution was aspirated, centrifuged at 1685 × *g* for 5 min, and resuspended in 0.85% (w/v) NaCl solution, and 1 mL of a certain dilution of the resuspended solution was added to 25 mL of PBS. The concentration of cells in the working solution was 2×10^6–4×10^7 CFU/mL.

2.2. High-intensity ultrasonic (HIU) treatment

An ultrasonic cell disintegrator (SCIENTZ-IID, maximum power 900 W, Xinzhi Biotechnology Co., Ltd., Ningbo, China) was used to apply different power and treatment time. The probe diameter was 6 mm, the operating depth was 10 mm, the treatment temperature was 25 °C, and the pulse interval was 3 s on/3 s off until completion[15]. Untreated *B. subtilis* was used as a negative control and placed in an ice bath for 4 h for further analysis. Before and after each experiment, the ultrasound probe was disinfected with 75% ethanol to avoid contamination of the samples. After sonication, the 50 mL conical flask was removed and immediately sealed to prevent microbial contamination from the air. The power density of ultrasound (D, W/mL) was from the equation D = P/V, where P is the input power and V is the volume of the medium[16].

2.3. Counting of cultivable B. subtilis cells

Cultivable *B. subtilis* cells were counted using a standard plate counting method[9]. Untreated and HIU-treated samples (90 W, 180 W, 270 W, 360 W; 5 min, 15 min, 25 min) were serially (1:10) diluted with 0.85% (w/v) NaCl solution and grown on plate count agar (PCA). Duplicate samples were analyzed. The petri dishes were incubated at 37 °C for 24 h, and then colony counting was performed. The log(N) of the residual count was calculated to determine the inactivation effect, where N (CFU/mL) is the number of residual counts after treatment.

2.4. Scanning electron microscopy observation of B. subtilis

After HIU treatment (90 W, 25 min; 270 W, 15 min; 360 W, 5 min), the *B. subtilis* suspensions were centrifuged at 6790 × *g* for 10 min at 4 ℃; subsequently, the bacterial precipitate was collected and washed three times with PBS buffer. Then, 1 mL of 2.5% glutaraldehyde solution was added to fix the bacterial precipitate for 12 h at 4 ℃, followed by dehydration in a graded ethanol series (30%, 50%, 70%, 80%, and 90% ethanol; 20 min for each gradient), and finally dehydrated twice with 100% ethanol. The dehydrated bacterial precipitate was suspended in ethanol, and 10 μL was aspirated onto slides and air-dried. The slide was cut, fixed on the metal carrier plate, and spray gold treatment was performed. After preparation, the surface changes in *B. subtilis* were observed using a scanning electron microscope (SEM; Thermo Scientific Apreo 2C, Thermo Fisher Scientific Co., China). Each sample was imaged three times, with typical images presented in the results.

2.5. Determination of intracellular protein leakage of B. subtilis

The intracellular protein exudation of *B. subtilis* after HIU treatment (90 W, 25 min; 270 W, 15 min; 360 W, 5 min) was evaluated. The bacterial suspension supernatant after HIU treatment was concentrated 100-fold using an ultrafiltration tube (3000 Da molecular weight cut-off, Merck KGaA, Darmstadt, Germany), and the protein concentrate of the retentate was determined using a Bradford Protein Assay Kit (Biyuntian Biotechnologies Co., Ltd., Shanghai, China) [17]. The assay was repeated five times for each sample. The concentrated retentates were also analyzed by SDS-PAGE in accordance with our previously reported procedure[18]. The SDS-PAGE analysis was repeated three times, and representative images were presented.

2.6. Determination of ATP content

The intracellular ATP content of *B. subtilis* after HIU treatment (90 W, 25 min; 270 W, 15 min; 360 W, 5 min) was measured using an enhanced ATP assay kit (Biyuntian Biotechnology Co., Ltd., Shanghai, China). The quantitative determination of ATP is a fluorescence-based method in which the assay enzymes catalyze the oxidation of firefly luciferin, which requires ATP. Chemiluminescence values were measured using a multifunctional enzyme marker (Synergy HTX, BioTek Instruments, Inc., Winooski, VT, USA). The assay was repeated three times for each sample.

2.7. Label-free quantitative proteomic analysis

2.7.1. Protein extraction and digestion

B. subtilis (untreated or HIU-treated) was lysed with lysis solution (1.5% SDS, 100 mM Tris-HCl, pH 8.1) and total protein was recovered by acetone precipitation. A complex solution (8 M Urea, 100 mM Tris-HCl) was added to the total protein precipitate and incubated with dithiothreitol for 1 h at 37 °C; subsequently, iodoacetamide (IAA, 40 mM) was added to alkylate the sulfhydryl group, and 100 mM Tris-HCl solution was added to the reduced, alkylated sample to dilute the urea concentration to below 2 M. The protein concentration was determined using the Bradford assay, and equal amounts of protein were used in the subsequent digestion and analysis[19]. Trypsin was added at an enzyme: protein mass ratio of 1:50 and incubated overnight at 37 °C for digestion. The next day, trifluoroacetate was added to terminate the digestion, and, finally, the supernatant was desalted using a Sep-Pak C_{18} column.

2.7.2. LC–MS/Ms

Mass spectrometric data were acquired using an Orbitrap Exploris 480 mass spectrometer in tandem with an EASY-n LC 1200 liquid phase LC–MS/MS system. The peptide samples were separated by an analytical column (75 μm × 25 cm, C_{18}, 1.9 μm, 100 Å). Two mobile phases (mobile phase A: 0.1% formic acid and mobile phase B: 0.1% formic acid, 80% ACN) were used to establish the analytical gradient: 0.0–68.0 min, 6%–25% mobile phase B; 68.0–84.5 min, 25%–45% B; 84.5–85.0

min, 45%–80% B; 85.0–92.0 min, 80% B. A flow rate of 300 nL/min was used[20]. The separated peptides were ionized by a nano-electrospray ion source (2.3 kV). The mass spectra were acquired in data- dependent acquisition mode, with each scan cycle containing one full MS scan (resolution, 60 K; automatic gain control, 300%; maximum injection time, 20 ms; scan range, 350–1500 *m/z*), and 20 subsequent MS/MS scans (resolution, 15 K; automatic gain control, 100%; maximum injection time, auto; cycle time, 2 s). The higher-energy C-trap dissociation collision energy was set to 30%. The screening window of the quadruple bar was set to 1.6 Da. The dynamic exclusion time for ion duplicate acquisition was set to 35 s[21]. The experiment was repeated three times for each treatment.

2.7.3. Data processing

The mass spectrometry data were searched using MaxQuant (V1.6.6) software; the database search algorithm used was Andromeda. The database used for the search was UniProtKB (*B. subtilis* (strain 168) [224308], date: 20210309). The main search parameters were: oxidation (M), acetyl (protein N-terminal), deamidation (NQ) for variable modifications; carbamidomethyl (C) for immobilization modifications; trypsin/P for enzymatic digestion; primary mass spectrometry matching tolerance of 20 ppm in the initial search and 4.5 ppm in the primary search; secondary mass spectrometry matching tolerance of 20 ppm. The search results were filtered by 1% false discovery rate at the protein and peptide level[22].

To study the function of the proteins, the functional database annotation of the identified proteins was performed using BLAST comparison (blastp, e-value $\leq 1e^{-5}$) for the Gene Ontology (GO) and Kyoto Encyclopedia of Genes and Genomes (KEGG) database annotation, and MultiLoc2 (https://abi-services.informatik.uni-tuebingen.de/multiloc2/webloc.cgi) for subcellular localization prediction[23–25].

Based on the quantification results, PCA analysis was performed to assess the biological replicates within groups and sample differences between groups. The ratio of the mean value of each protein across all biological replicates was quantified as the fold difference (fold change [FC]), and an FC of ≥ 1.5 was selected, and a *t*-test was performed to select P-values of < 0.05, which indicated significant differences between groups.

2.8. Statistical analysis

The study data were expressed as the mean and standard deviation (mean ± standard deviation). The statistical analysis was performed by one-way analysis of variance using GraphPad Prism 8.0 software, and differences were considered significant at $p < 0.05$.

3. Results

3.1. Inhibitory effect of HIU treatment on B. subtilis

The number of cultivable *B. subtilis* cells after HIU treatment was calculated using a standard plate counting method. After treatment, the number of cultivable *B. subtilis* cells was decreased, and continued to decrease as the treatment time increased, and the slope (absolute value) of the curve of the number of colonies increased as the ultrasonic power increased (Fig. 1). The number of cultivable *B. subtilis* cells was decreased by approximately 1.54 logarithms after treatment at 360 W for 25 min, indicating efficient inhibition.

To evaluate the inhibitory effect and the associated mechanism of ultrasound treatment on *B. subtilis*, the HIU treatments of 270 W for 15 min (US-270, D = 10.38 W/mL, 1.01 log decrease), 90 W for 25 min (US-90, D = 3.46 W/mL, 0.49 log decrease), and 360 W for 5 min (US-360, D = 13.85 W/mL, 0.47 log decrease) were selected, and their effects were compared and analyzed.

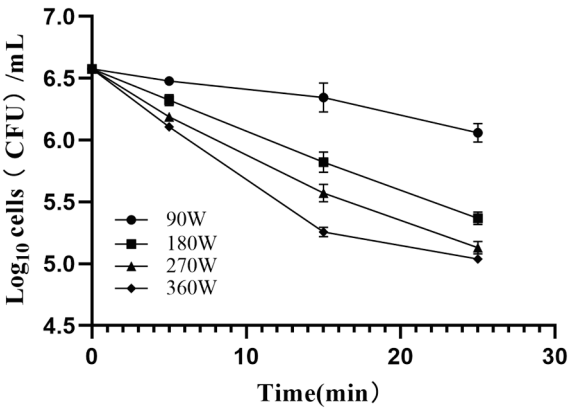

Fig. 1. Changes in the number of cultivable *B. subtilis* colonies after application of different ultrasonic treatments (different power and time).

3.2. Changes in B. subtilis surface structure after HIU treatment

The structural damage to the surface of *B. subtilis* vegetative cells after HIU treatment was observed by SEM. Most of the *B. subtilis* vegetative cells in the untreated group (CK) were rod-shaped with intact, flat, and smooth surface morphology. Compared with the CK group, ultrasound treatment caused cell surface wrinkling, fissures, and pore formation (Fig. 2 A–D). Wrinkling was observed after the US-90, US-270, and US-360 treatments, but it was most obvious after the US-90 treatment; in contrast, cracks and pore formation appeared mainly after the US-270 and US-360 treatments and were not observed after the US-90 treatment. In addition, greater adhesion between cells was observed in HIU-treated *B. subtilis*, which indirectly reflected the changes and destruction of the cell structure.

3.3. Intracellular protein exudation of B. subtilis after HIU treatment

Wrinkles and cracks on the surface of *B. subtilis* vegetative cells may cause the leakage of intracellular material. Therefore, the protein content in the supernatant of the bacterial suspension was determined. In the untreated *B. subtilis* suspension supernatant concentrate (100 ×), the protein concentration was extremely low (0.34 μg/mL). These trace proteins are likely to be exocrine proteins produced by the normal physiological activities of *B. subtilis*. Compared with the untreated group, the protein concentrations in the *B. subtilis* suspension supernatant were over ten times more concentrated after US-90 and US-360 treatment, at 3.28 μg/mL and 2.98 μg/mL, respectively. After US-270 treatment, the protein concentration was further increased to 5.40 μg/mL (Fig. 2E). The amount of intracellular protein leakage caused by ultrasound treatment was positively correlated with the decrease in the number of cultivable *B. subtilis* cells: US-270 treatment resulted in a 1.01 log decrease and the greatest protein leakage (5.40 μg/mL); the US-90 and US-360 treatments resulted in a similar decrease (0.49 log) and a similar degree of protein leakage. This indicated that the destruction of the cell wall/membrane and the intracellular protein leakage caused by ultrasound are the major reasons why *B. subtilis* could not be cultured. The SDS-PAGE profile, which provides a more intuitive indication of the different degrees of intracellular protein leakage, was consistent with the protein concentration results (Fig. 2F).

3.4. Changes in intracellular ATP content of B. subtilis after HIU treatment

The destruction of the cell wall/membrane structure and the disturbance of the cytoplasm by HIU treatment result in severe disturbance of the intracellular physiological activities of *B. subtilis*. The content of intracellular ATP is an important indicator that can reflect the

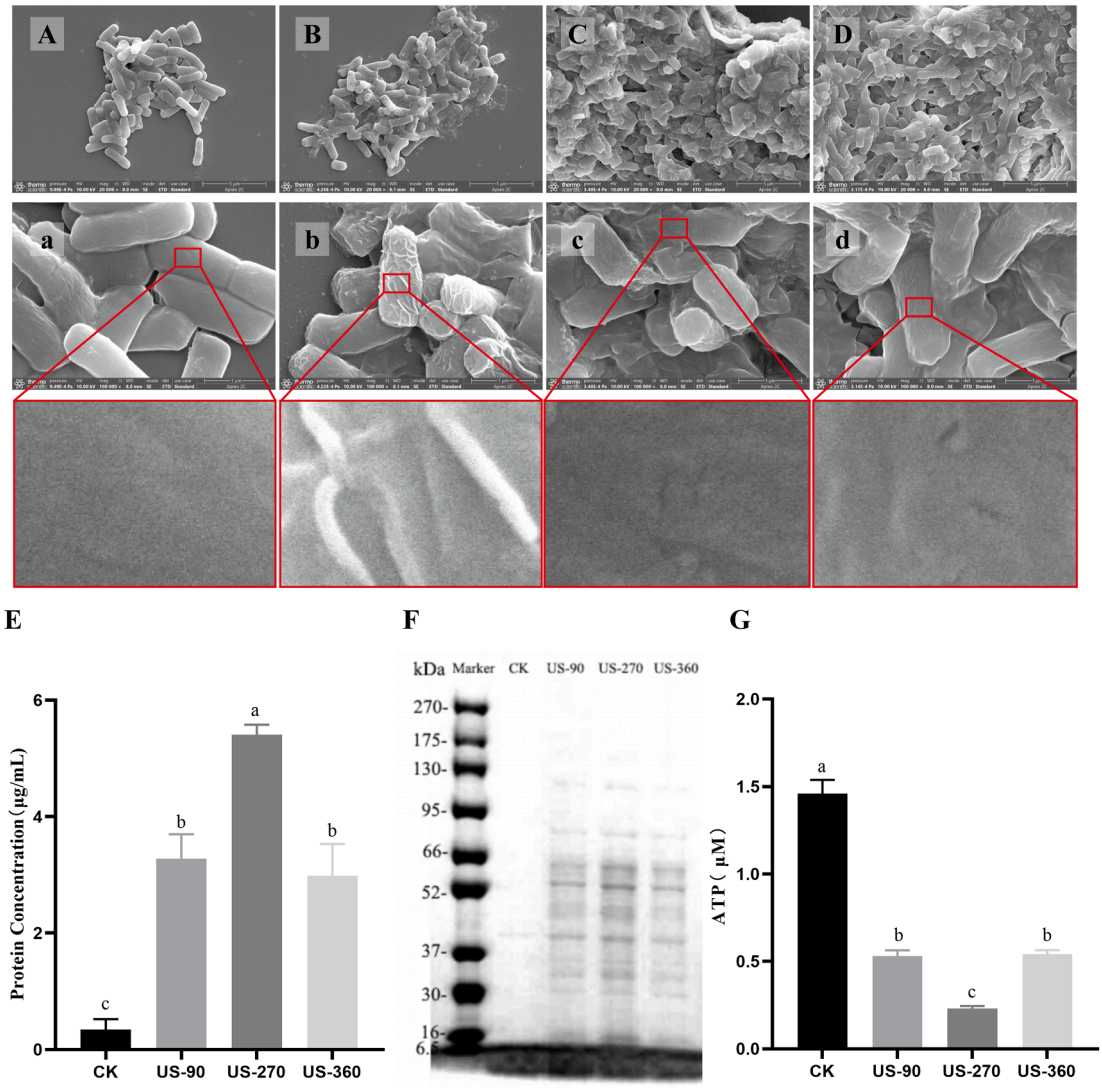

Fig. 2. Changes in *B. subtilis* after high-intensity ultrasound (HIU) treatment. A–D, SEM images of untreated *B. subtilis* (CK; A, a), treated with 90 W for 25 min (US-90; B, b), treated with 270 W for 15 min (US-270; C, c), and treated with 360 W for 5 min (US-360; D, d); E, the protein content in the supernatant of the *B. subtilis* suspension after HIU treatment; F, the SDS-PAGE of the supernatant of the *B. subtilis* suspension after HIU treatment; G, the intracellular ATP content of *B. subtilis* after HIU treatment.

physiological activity of bacteria[8]. In this study, compared with the untreated group (CK, 1.46 μM), the intracellular ATP content was decreased significantly after HIU treatment (Fig. 2G). The US-270 treatment resulted in the greatest decrease (of 84.22%); after the US-90 and US-360 treatments, the intracellular ATP content decreased to 0.54 and 0.56 μM, respectively.

3.5. Quantitative proteomic analysis of *B. subtilis* after HIU treatment

3.5.1. Comparison of protein profiles

In total, 2087 proteins were identified from *B. subtilis* in this study. The overall comparison of the proteomes was performed by principal component analysis, and the results identified differences between the CK, US-90, US-270, and US-360 groups (Fig. 3A). The principal component 1 (PC1) and principal component 2 (PC2) values of the four groups were 36.37% and 17.01%, respectively. The distribution of the four groups on the PCA plots showed separation, especially in the PC1 dimension. Therefore, the distribution of samples on the PC1 dimension was replotted (Fig. 3B). The US-90 group was more connected to the US-360 group than the CK group and the US-270 group (PC1 score: US-270 > US-90 ≈ US-360 > CK). These results suggested that the changes in the *B. subtilis* protein profiles caused by HIU were correlated with the degree of lethality.

Pairwise comparisons between groups were performed, and 209 differentially expressed proteins (DEPs) were identified after screening (FC > 1.5 or FC < 0.67, and $p < 0.05$; Table S1). As shown in Fig. 3C, the largest number of DEPs was found for the comparison between the US-270 and CK groups (181 DEPs), with only five DEPs found between the US-90 and US-360 groups. These results were consistent with the PCA analysis. In the pairwise comparison between the three ultrasound treatment groups and the CK group, 14 DEPs overlapped (Fig. 4D). These 14 DEPs were the common response proteins of *B. subtilis* to different ultrasonic treatments; these proteins are important for understanding the inhibitory mechanism of HIU treatment on *B. subtilis*, and may be potential indicators of sonicated *B. subtilis*.

3.5.2. Subcellular distribution of DEPs

After transcription and translation, proteins are synthesized by the ribosome and transported to specific subcellular regions and localization, where they perform their specified function. Therefore, the annotation of the subcellular localization of DEPs can provide important information on their function. Among the 2087 identified *B. subtilis*

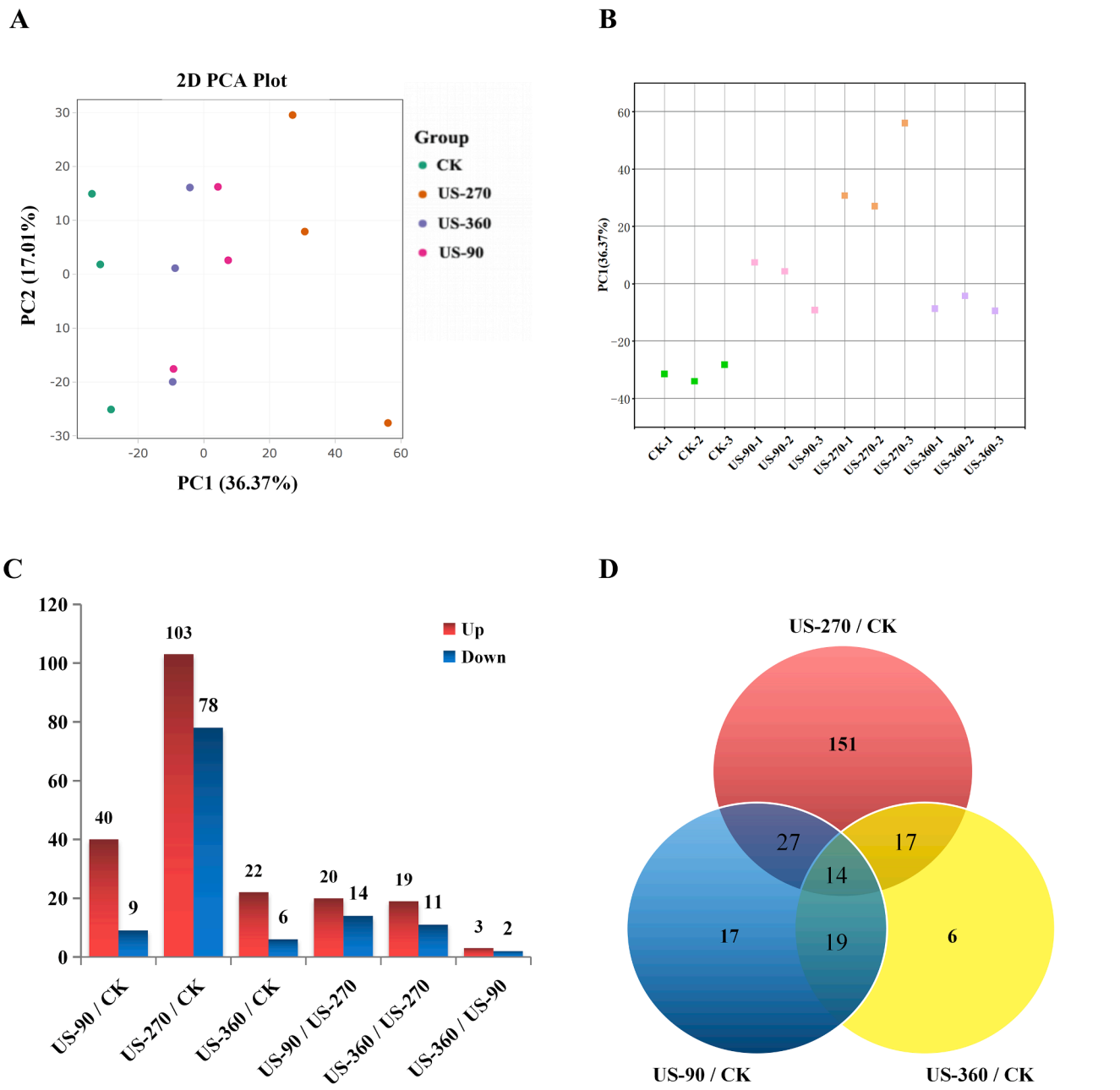

Fig. 3. Quantitative proteomic analysis of *B. subtilis* after high-intensity ultrasound (HIU) treatment. A, The principal component analysis of the protein profiles of *B. subtilis* after different HIU treatments; B, Distribution of principal component 1; C, The number of DEPs in the pairwise comparison between groups; D, Venn diagram of differentially expressed proteins (DEPs) after HIU treatment. CK, untreated group; US-90, 90 W for 25 min; US-270, 270 W for 15 min; US-360, 360 W for 5 min.

proteins, 1824 were annotated. The location was annotated as "cytoplasmic membrane" for 23.68% of these proteins and "cytoplasmic" for 74.00%. In comparison, the DEPs of *B. subtilis* induced by HIU treatment were mostly localized on the "cytoplasmic membrane", accounting for 49.29%–72.73% of the total DEPs (Fig. 4A). It is worth noting that only 20 of the identified *B. subtilis* proteins were annotated to be located on the "cell wall", but many of them were differentially expressed after HIU treatment. These results suggested that the "cytoplasmic membrane" and "cell wall" of *B. subtilis* were the parts that were most changed after HIU treatment. This was consistent with the results observed by SEM. In addition, the second-most common annotation for the DEPs after HIU treatment was "cytoplasmic".

3.5.3. GO annotation and analysis of DEPs

GO analysis was performed to classify the functions of 209 DEPs of *B. subtilis* induced by HIU treatment. As shown in Fig. 4B, in the "biological process" category, the DEPs after HIU treatment were mainly classified into nine terms, among which "cellular process", "metabolic process", "localization", "biological regulation", and "locomotion" were dominant. The terms "localization" and "locomotion" were of particular interest because the number of upregulated DEPs was far higher than that of the downregulated DEPs. For the "molecular function" category, DEPs were mainly classified into 10 terms, which were dominated by "catalytic activity", "binding", and "transporter activity".

3.5.4. KEGG enrichment analysis of DEPs

To identify the potential regulatory pathways for the DEPs of

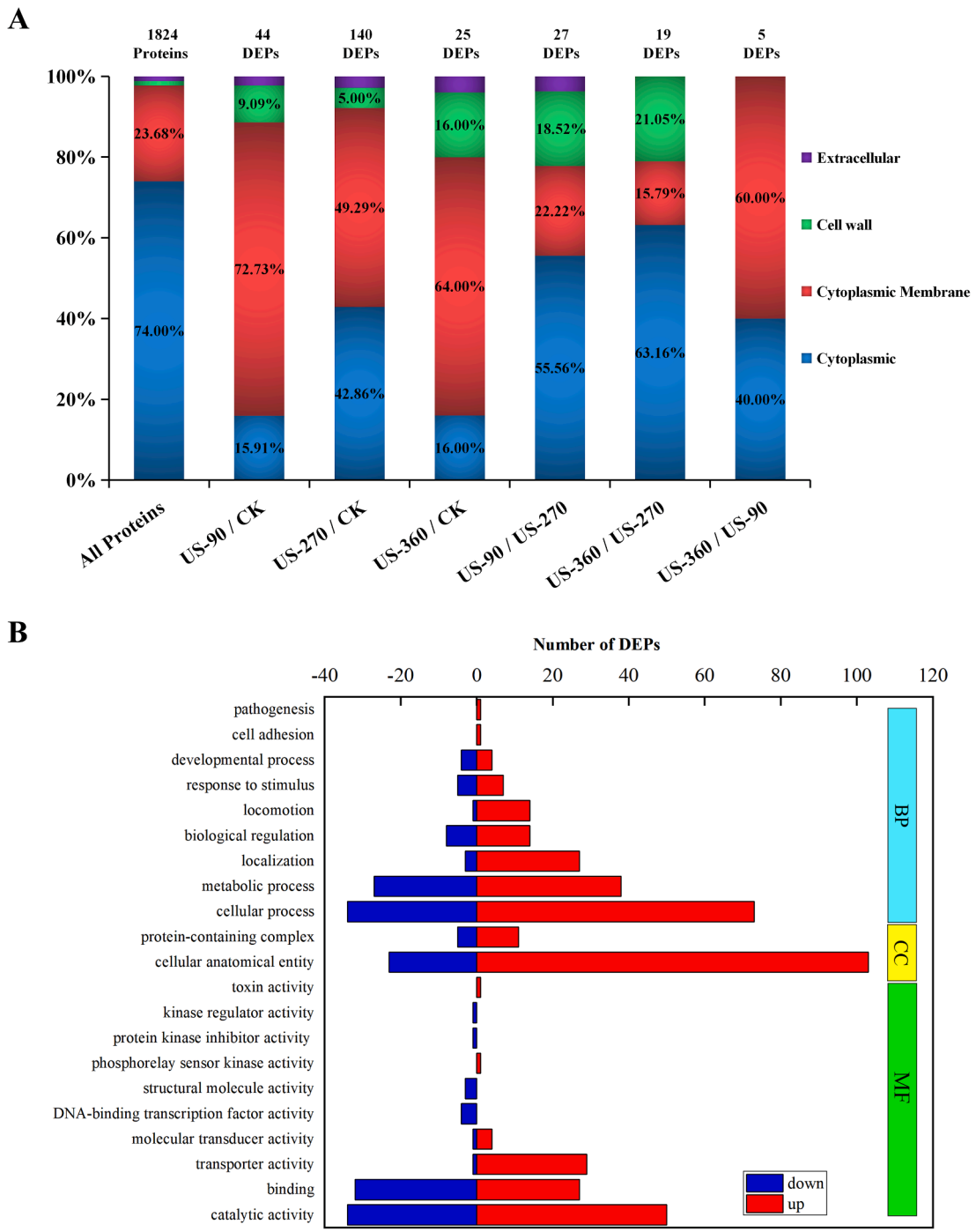

Fig. 4. Subcellular distribution (A) and GO analysis (B) of differentially expressed proteins (DEPs) after high-intensity ultrasound (HIU) treatment. CK, untreated group; US-90, 90 W for 25 min; US-270, 270 W for 15 min; US-360, 360 W for 5 min.

B. subtilis induced by HIU treatment, KEGG enrichment analysis was performed. Compared with the CK group, the DEPs in *B. subtilis* in the US-90 group were annotated to 23 KEGG pathways, of which "bacterial chemotaxis" (5 DEPs, p.adjust < 0.01) and "two-component system" (7 DEPs, p.adjust < 0.01) were significantly enriched (Table S2). In the comparison between the US-270 and CK groups, 181 DEPs were annotated to 50 KEGG pathways, of which two pathways were significantly enriched: "bacterial chemotaxis" (7 DEPs, p.adjust < 0.05) and "oxidative phosphorylation" (8 DEPs, p.adjust < 0.05). In total, three KEGG pathways were enriched with 28 DEPs in the comparison between the US-360 and CK groups: "bacterial chemotaxis" (4 DEPs, p.adjust < 0.01), "flagellar assembly" (3 DEPs, p.adjust < 0.05), and "cationic antimicrobial peptide (CAMP) resistance" (2 DEPs, p.adjust < 0.05). Notably, "bacterial chemotaxis" was the KEGG pathway that was commonly enriched, and all the DEPs involved in this pathway were upregulated in *B. subtilis* after HIU treatment.

4. Discussion

4.1. Bacteriostatic effects of HIU treatment on B. subtilis vegetative cells

In this study, HIU treatment caused notable inhibition of *B. subtilis* vegetative cells, and the degree of inhibition was positively correlated with the power and time of ultrasonic treatment. These results were

similar to those of previous studies. Researchers found that *A. flavithermus* decreased by 4.26 log after sonication for 10 min in optimal conditions and that *B. coagulans* decreased by 4.53 log; the log reduction of both *Bacillus* species increased significantly with longer sonication times[14]. In contrast, Yu et al. found that ultrasound at 60 W and 10 min treatment killed only<0.1 log of *Staphylococcus aureus*; this may have been due to the protective effect of the biofilm on bacteria, which mitigates the direct lethal effect of ultrasound[26]. Therefore, the bacteriostatic effect of ultrasound on bacterial cells will vary with the bacterial species, the status of the bacteria, and the ultrasound intensity and application time. Generally, a "marginal utility" of the ultrasonic intensity and ultrasonic time on the bacterial inhibitory effect was observed: that is, the inhibition efficacy was reduced at a high power and over a long application time.

As the above mentioned study found, ultrasound usually only results in bacterial inhibition and partial sterilization; this cannot effectively ensure the safety of food and has limited the application of ultrasound in food processing. However, several recent studies have found that ultrasound, in combination with other bacteriostatic agents, could enhance the disinfection of *Staphylococcus aureus, Salmonella typhimurium*, and other bacteria[9,27]. Therefore, further study to confirm the inhibitory effect of HIU combined with antibacterial agents on *B. subtilis* is of value. Moreover, in some studies, it has been found that ultrasound could improve the functional properties of food. For example, the foaming properties of egg white proteins were enhanced after ultrasound treatment[28]. Therefore, the application of ultrasound in certain foods would confer multiple benefits.

The transient cavitation effect induced by HIU and the accompanying shock waves and liquid jets causes the perforation and rupture of the bacterial cell wall/membrane; this is generally considered to be the main mechanism of ultrasound-induced bacterial damage[29]. A previous study reported that ultrasound treatment had strong mechanical destructive effects on both nutrient cells and spores of some *Bacillus* species[14]. Similar effects were also found in this study (Fig. 2B–D).

HIU treatment may expose teichoic acid in the cell wall and enhance the adhesion between *B. subtilis* cells, as was observed in the SEM images. In addition to the damage to the cell structure of *B. subtilis* caused by HIU treatment, leakage and dissolution also occurred. In this study, the amount of protein leakage caused by HIU treatment was positively correlated with the decrease in the number cultivable *B. subtilis* cells. Although the amount of protein leakage was significantly different between the HIU treatment groups, the SDS-PAGE profile showed that the types of leaked protein may be similar. The composition of protein leakage induced by ultrasonic treatment is worthy of attention and further study, as it will help to elucidate the bacteriostatic mechanism of ultrasound.

HIU treatment not only causes mechanical damage to *B. subtilis*, but may also disrupt its cytoplasm owing to its strong penetration, even leading to the disintegration of some enzyme complexes. In this study, it was found that ultrasonic treatment caused variable decreases in the intracellular ATP content of *B. subtilis*, and the decrease in ATP was closely related to the decrease in the number of cultivable cells. Similar findings have been reported in previous studies. In the study of Li et al., both low- and high- intensity sonication for 25 min resulted in a significant decrease in ATP levels in *E. coli* cells[10]. Another report also found that the ATP content in *E. coli O157:H7* cells was reduced by approximately 2.18-fold after sonication (100 W, 4 min) compared with the untreated group[8]. The ATP content is an overall response to the level of intracellular physiological activity. Therefore, the large change in ATP content after ultrasonic treatment is an indication of significant disturbance in the intracellular physiological activity of *B. subtilis*. To explore the regulatory mechanisms of *B. subtilis* in response to HIU treatment, quantitative proteomic analysis was performed.

4.2. Regulatory mechanisms of *B. subtilis* in response to HIU treatment

The bacteriostatic mechanism of ultrasound on *B. subtilis* cells is mediated through two mechanisms: the damage caused by HIU treatment to *B. subtilis* and the response of *B. subtilis* to ultrasound stress. However, bacteria have evolved many complex regulatory networks to counteract stress and repair damage caused by adverse natural stress conditions (such as cold, heat, pH, oxidation, osmotic pressure, UV radiation, and pulsed electric fields)[30]. Therefore, quantitative proteomic analysis was conducted to explore the relevant regulatory pathways of *B. subtilis* in response to ultrasound stress.

The cell wall and membrane are the interface between *B. subtilis* and the external environment for signal and substance exchange. On the plasma membrane, the ATP-binding cassette transporter (ABC) is the key to ensuring the orderly influx and efflux of substances[31,32]. In the present study, after the US-90, US-270 and US-360 treatments, many proteins related to the ABC transporter were upregulated. These proteins were mainly involved in the manganese transport system (MntA, MntB, MntC), the zinc transport system (ZnuA, ZnuC), the oligopeptide transport system (OppA, OppC), the methionine transport system (MetP, MetQ, MetN), L-cystine transport system (TcyA, TcyB, TcyC), the glycine betaine/carnitine/choline transport system (OpuAA, OpuAB, OpuAC, OpuCA, OpuCC), the melibiose/tartarose/starch transport system (MelC, MelD, MelE), the maltose transport system (MdxE, MdxF), and oligosaccharide and galacto-oligosaccharide transporter systems (Fig. 5A). This upregulation of ABC transporter-related proteins could promote the uptake of nutrients and other molecules and enhance the membrane transport function of *B. subtilis*, which would, in turn, enhance its survival under ultrasound stress. Similar results were reported in a previous study, which found that the expression of the phosphate transporter ATP-binding protein was upregulated in *B. cereus* spores after ultrasound treatment, indicating an enhanced phosphate transport capacity[33]. In addition, the upregulation of these ABC transporter-related proteins was positively correlated with the lethal effect caused by ultrasound.

In addition to the transport of substances, the response of *B. subtilis* to ultrasound stress is also reflected in the regulation of signal transduction. The two-component system is the most important signal transduction system that bacteria use to perceive and adapt to the environment. The structure of this system is highly conserved among different bacteria, and histidine kinases are the core proteins of this system. In the present study, it was found that histidine kinases of *B. subtilis* were upregulated after ultrasound treatment, including DegS, WalK, CssS, GlnK, ResE, MalK, and YclK (Fig. 5B). One of these proteins, DegS (upregulated 1.16–1.28-fold after ultrasound treatment), plays an important role in the production of degradative enzymes, flagellar formation, and biofilm formation. By acting as both a protein kinase and a protein phosphatase, DegS not only performs autophosphorylation and the subsequent transfer of phosphate to DegU, but also dephosphorylates DegU[34]. The sensor histidine kinase WalK, which is involved in the regulation of the ftsAZ, tagAB, and tagDEF operons[35], was significantly upregulated ($p < 0.05$) in *B. subtilis* treated with US-90 and US-360. In addition, other sensor transduction proteins (BceR, YvaQ, and YfmS) were upregulated, which would accelerate the adaptation to extracellular changes through the regulation of methylation levels. In summary, in response to ultrasound stress, some key proteins of the two-component regulatory system of *B. subtilis* were upregulated. This upregulation would enhance cell sensitivity to changes in the external environment and allow more rapid transmission of signals to regulatory protein components located in the cytoplasm, facilitating resistance to ultrasound stress.

The survival of any organism is dependent on the effective provision of energy, especially after ultrasound treatment; all types of stress responses require a large amount of energy to maintain, and the most important link in the provision of energy in bacterial cells is the tricarboxylic acid (TCA) cycle. In the present study, all HIU treatments caused

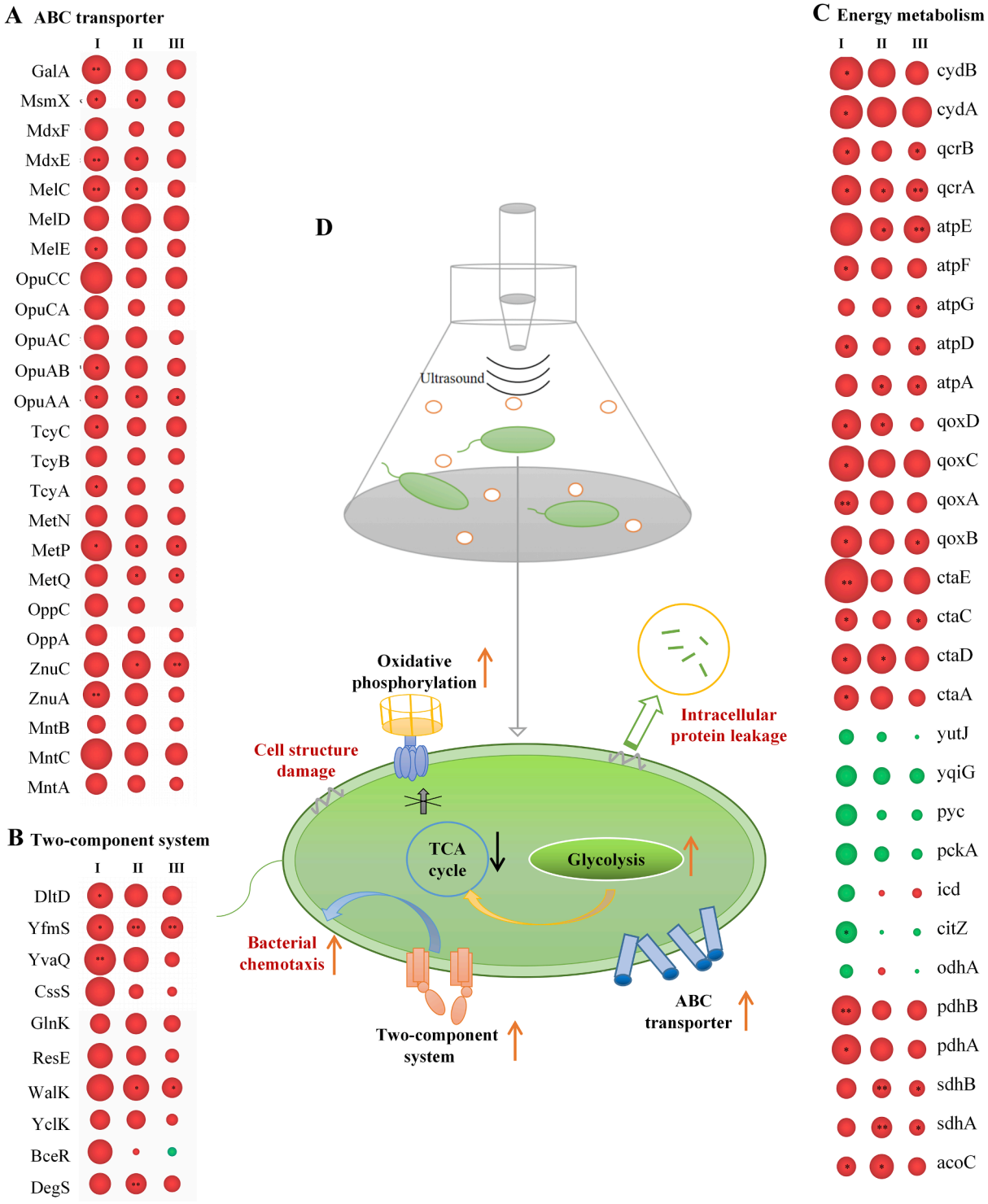

Fig. 5. Regulatory mechanisms of *B. subtilis* in response to high-intensity ultrasound (HIU) treatment. A, Changes in the expression of proteins associated with the ABC transporter after HIU treatment; B, Changes in the expression of proteins associated with the two-component system after HIU treatment; C, Changes in the expression of proteins associated with energy metabolism after HIU treatment. CK, untreated group; US-90, 90 W for 25 min; US-270, 270 W for 15 min; US-360, 360 W for 5 min. I, US-270/CK; II, US-90/CK;III, US-360/CK. Inside the circle, * indicates $p < 0.05$,** indicates $p < 0.01$.

downregulation of the expression of key proteases related to the TCA cycle, such as citrate synthase, which controls the entrance to the TCA cycle and plays a key role in all subsequent reactions. Compared with US-90 treatment, US-270 and US-360 treatments caused more downregulation of TCA cycle-related proteins, such as isocitrate dehydrogenase. It could also be inferred that HIU causes downregulation of key TCA cycle-related proteins that was closely related to ultrasound power (Fig. 5C).

With close links to the TCA cycle, the oxidative phosphorylation pathway is the main source of ATP generation in organisms. Most of the oxidative phosphorylation related-proteins were upregulated, to different degrees, after HIU treatment. The upregulation of cytochrome *c* oxidase may lead to an increase in transmembrane proton pumping capacity and electron consumption rate, whereas the upregulation of

ATP synthase suggested that HIU treatment may induce greater ATP production. Therefore, *B. subtilis* cells may try to respond to the reduction in proton gradient accumulation through the upregulation of ATP synthase, but this does not alleviate the overall decreasing trend in intracellular ATP content owing to the downregulation of the upstream TCA cycle. This was also consistent with the ATP content assay, which showed a decrease in intracellular ATP content after HIU treatment.

Similar regulatory responses were reported in previous studies of *E. coli* treated with sonication[8,33]. However, the decrease in ATP content was sharp, which appeared to be mismatched with the regulation of protein expression related to energy metabolism. This was probably due to the breakdown of the enzyme complex and the disturbance of cell homeostasis induced by ultrasound. As a prokaryote without organelles, orderly physiological processes are realized through the mesosome, local accumulation of substances, and the condensate of proteins in the bacterial cytoplasm[36]. Obviously, HIU could affect the physiological process of *B. subtilis* by disturbing its intracellular homeostasis, especially the multi-step physiological processes of the TCA cycle and oxidative phosphorylation.

In addition to the main effects of HIU treatment on substance transport, signal transduction, and energy metabolism in *B. subtilis*, several other physiological activities were affected. For example, by upregulating the methyl-accepting chemotactic proteins TlpB, TlpC, McpA, McpB, McpC, flagellin FliL, motor protein A, and swarm motility proteins SwrC and SwrD, the cells can move towards an environment more conducive to their survival and thus take up relevant nutrients and essential components. In addition, it was found that key phosphorylation-related proteins that regulate the initiation of spore development, spore-initiating phosphotransferases B and F, were downregulated by ultrasound treatment. Sporogenic acid kinase C, which is involved in the phosphorylation of spore-regulating protein spo0A, was significantly upregulated, indicating that ultrasound treatment had an effect on spore formation in *B. subtilis*. Moreover, peptidoglycan hydrolysis-related enzymes responsible for local hydrolysis of the cell wall, such as peptidoglycan endopeptidase LytE, endonuclease YhcR, D-glutamyl-m-diaminopyrimidine endopeptidase CwlS, and amidase enhancer, were upregulated by ultrasound treatment. This may, to some extent, indicate that cell division is accelerated by sonication as a response to the unfavorable external environment; however, this increases the risk of apoptosis.

In this study, the bactericidal effect of HIU on *B. subtilis* was studied at the laboratory scale; its industrial application would be difficult as the HIU power density used was relatively high (3.46–13.85 W/mL). However, there are two potential routes for industrial-scale HIU sterilization. One method is the reduction of the HIU power density by combination with natural antibacterial or other non-thermal processing technologies. For example, Bi et al. applied HIU treatment and lysozyme to liquid whole egg, and found that it not only significantly inactivated *Salmonella typhimurium* but also improved the color and heat resistance of liquid whole egg[9]. In addition, HIU is used in the processing of some high-value foods, such as micro/nano emulsions for the delivery of food functional ingredients, ultrasound-assisted enzymatic hydrolysis preparation of functional peptides, and ultrasound-assisted modification of food macromolecules[37,38]. These functional foods are usually heat-sensitive, and the processing capacity is usually small. Therefore, the inactivation of potentially contaminating microorganisms could be accompanied by ultrasonic processing without additional cost. This study provides part of the foundation for the future exploration, improvement, and application of ultrasonic sterilization.

5. Conclusion

The results of this study showed that HIU had a notable inhibitory effect on the number of cultivable *B. subtilis* cells. The SEM images, SDS-PAGE profiles, and intracellular ATP content analysis suggested that HIU treatment disrupted the normal activities of *B. subtilis* mainly by damaging the cell surface structure, leading to the leakage of intracellular proteins, and blocking energy metabolism and ATP production. The damage caused by HIU treatment varied with the intensity and time applied, but was positively correlated with the degree of lethality caused by HIU. Moreover, many proteins in *B. subtilis* were differentially expressed in response to HIU stress. *B. subtilis* attempted to survive by enhancing substance intake (upregulating the ABC transporter), environmental perception (upregulation of the two-component system), and ATP production (upregulation of oxidative phosphorylation), but the structural damage and blocked TCA cycle caused these restorative actions to be unsuccessful. These findings are helpful for an understanding of the bacteriostatic mechanism of HIU on *B. subtilis*. In further studies, combining HIU with natural antibacterial agents or other non-thermal sterilization technologies for the inactivation of *B. subtilis* is expected to achieve better results. A suitable application is in high-value, heat-sensitive, HIU-processed foods, such as micro/nano emulsions that are used for the delivery of food functional ingredients.

CRediT authorship contribution statement

Wei Luo: Investigation, Data curation, Formal analysis, Writing – original draft. **Jinqiu Wang:** Methodology, Resources, Writing – review & editing, Project administration. **Yi Wang:** Investigation. **Jie Tang:** Writing – review & editing. **Yuanhang Ren:** Methodology, Resources. **Fang Geng:** Conceptualization, Writing – original draft, Writing – review & editing, Supervision, Funding acquisition.

Declaration of Competing Interest

The authors declare that they have no known competing financial interests or personal relationships that could have appeared to influence the work reported in this paper.

Acknowledgments

This work was supported by the National Natural Science Foundation of China (31970092, 32102254, 32072236) and Sichuan Science and Technology Program (2021YJ0477).

Appendix A. Supplementary data

Supplementary data to this article can be found online at https://doi.org/10.1016/j.ultsonch.2021.105862.

References

[1] A.I. Delbrück, Y. Zhang, V. Hug, C. Trunet, A. Mathys, Isolation, stability, and characteristics of high-pressure superdormant Bacillus subtilis spores, Int. J. Food Microbiol. 343 (2021), 109088.
[2] N. Mtimet, C. Trunet, A.-G. Mathot, L. Venaille, I. Leguérinel, L. Coroller, O. Couvert, Modeling the behavior of Geobacillus stearothermophilus ATCC 12980 throughout its life cycle as vegetative cells or spores using growth boundaries, Food Microbiol. 48 (2015) 153–162.
[3] P. Setlow, Spores of Bacillus subtilis: their resistance to and killing by radiation, heat and chemicals, J. Appl. Microbiol. 101 (2006) 514–525.
[4] C. Trunet, N. Mtimet, A.G. Mathot, F. Postollec, I. Leguérinel, O. Couvert, F. Carlin, L. Coroller, Effect of incubation temperature and pH on the recovery of Bacillus weihenstephanensis spores after exposure to a peracetic acid-based disinfectant or to pulsed light, Int. J. Food Microbiol. 278 (2018) 81–87.
[5] C.M. Trunet, N. Mtimet, A.-G. Mathot, F. Postollec, I. Leguerinel, D. Sohier, O. Couvert, F.D.R. Carlin, L. Coroller, Modeling the Recovery of Heat-Treated Bacillus licheniformis Ad978 and Bacillus weihenstephanensis KBAB4 Spores at Suboptimal Temperature and pH Using Growth Limits, Applied, Environ. Microbiol. 81 (2014) 562–568.
[6] L. Fan, B.B. Ismail, F. Hou, A.I. Muhammad, T. Ding, D. Liu, Ultrasound pretreatment enhances the inhibitory effects of nisin/carvacrol against germination, outgrowth and vegetative growth of spores of Bacillus subtilis ATCC6633 in laboratory medium and milk: Population and single-cell analysis, Int. J. Food Microbiol. 311 (2019), 108329.
[7] R. Sevenich, A. Mathys, Continuous Versus Discontinuous Ultra-High-Pressure Systems for Food Sterilization with Focus on Ultra-High-Pressure Homogenization

and High-Pressure Thermal Sterilization: A Review, Comprehensive reviews in food science food safety 17 (3) (2018) 646–662.
[8] L. Lin, X. Wang, C. Li, H. Cui, Inactivation mechanism of E. coli O157:H7 under ultrasonic sterilization, Ultrasonics Sonochemistry 59 (2019) 104751, https://doi.org/10.1016/j.ultsonch.2019.104751.
[9] X. Bi, X. Wang, Y. Chen, L. Chen, Y. Xing, Z. Che, Effects of combination treatments of lysozyme and high power ultrasound on the Salmonella typhimurium inactivation and quality of liquid whole egg, Ultrasonics Sonochemistry 60 (2020), 104763.
[10] J. Li, L. Ma, X. Liao, D. Liu, X. Lu, S. Chen, X. Ye, T. Ding, Ultrasound-Induced Escherichia coli O157:H7 Cell Death Exhibits Physical Disruption and Biochemical Apoptosis, Front. Microbiol. 9 (2018).
[11] J. Li, X. Zhang, M. Ashokkumar, D. Liu, T. Ding, Molecular regulatory mechanisms of Escherichia coli O157:H7 in response to ultrasonic stress revealed by proteomic analysis, Ultrasonics Sonochemistry 61 (2020), 104835.
[12] R. Kaavya, R. Pandiselvam, S. Abdullah, N.U. Sruthi, Y. Jayanath, C. Ashokkumar, A. Chandra Khanashyam, A. Kothakota, S.V. Ramesh, Emerging non-thermal technologies for decontamination of Salmonella in food, Trends Food Sci. Technol. 112 (2021) 400–418.
[13] A. Tremarin, T.R.S. Brandão, C.L.M. Silva, Application of ultraviolet radiation and ultrasound treatments for Alicyclobacillus acidoterrestris spores inactivation in apple juice, LWT 78 (2017) 138–142.
[14] S.N. Khanal, S. Anand, K. Muthukumarappan, M. Huegli, Inactivation of thermoduric aerobic sporeformers in milk by ultrasonication, Food Control 37 (2014) 232–239.
[15] Y. Xie, J. Wang, Y. Wang, D. Wu, D. Liang, H. Ye, Z. Cai, M. Ma, F. Geng, Effects of high-intensity ultrasonic (HIU) treatment on the functional properties and assemblage structure of egg yolk, Ultrasonics Sonochemistry 60 (2020), 104767.
[16] J. Li, T. Ding, X. Liao, S. Chen, X. Ye, D. Liu, Synergetic effects of ultrasound and slightly acidic electrolyzed water against Staphylococcus aureus evaluated by flow cytometry and electron microscopy, Ultrasonics Sonochemistry 38 (2017) 711–719.
[17] F. Geng, Y. Xie, Y. Wang, J. Wang, Depolymerization of chicken egg yolk granules induced by high-intensity ultrasound, Food Chem. 354 (2021), 129580.
[18] J. Wang, J. Xiao, X. Liu, Y. Gao, Z. Luo, X. Gu, J. Zhang, D. Wu, F. Geng, Tandem mass tag-labeled quantitative proteomic analysis of tenderloins between Tibetan and Yorkshire pigs, Meat Sci. 172 (2021), 108343.
[19] F. Geng, Y. Xie, J. Wang, K. Majumder, N. Qiu, M. Ma, N-Glycoproteomic Analysis of Chicken Egg Yolk, Journal of agricultural food chemistry 66 (43) (2018) 11510–11516.
[20] X. Liu, J. Wang, Q. Huang, L. Cheng, R. Gan, L. Liu, D. Wu, H. Li, L. Peng, F. Geng, Underlying mechanism for the differences in heat-induced gel properties between thick egg whites and thin egg whites: Gel properties, structure and quantitative proteome analysis, Food Hydrocolloids 106 (2020), 105873.
[21] J. Wang, X. Liu, S. Li, H. Ye, W. Luo, Q. Huang, F. Geng, Ovomucin may be the key protein involved in the early formation of egg-white thermal gel, Food Chem. 366 (2022) 130596, https://doi.org/10.1016/j.foodchem.2021.130596.
[22] X. Liu, J. Wang, L. Liu, L. Cheng, Q. Huang, D. Wu, L. Peng, X. Shi, S. Li, F. Geng, Quantitative N-glycoproteomic analyses provide insights into the effects of thermal processes on egg white functional properties, Food Chem. 342 (2021) 128252, https://doi.org/10.1016/j.foodchem.2020.128252.
[23] M. Ashburner, C.A. Ball, J.A. Blake, D. Botstein, H. Butler, J.M. Cherry, A.P. Davis, K. Dolinski, S.S. Dwight, J.T. Eppig, M.A. Harris, D.P. Hill, L. Issel-Tarver, A. Kasarskis, S. Lewis, J.C. Matese, J.E. Richardson, M. Ringwald, G.M. Rubin, G. Sherlock, Gene Ontology: tool for the unification of biology, Nat. Genet. 25 (1) (2000) 25–29.
[24] M. Kanehisa, S. Goto, M. Hattori, K.F. Aoki-Kinoshita, M. Itoh, S. Kawashima, T. Katayama, M. Araki, M. Hirakawa, From genomics to chemical genomics: new developments in KEGG, Nucleic Acids Res. 34 (2006) D354–D357.
[25] P.L. Ross, Y.N. Huang, J.N. Marchese, B. Williamson, K. Parker, S. Hattan, N. Khainovski, S. Pillai, S. Dey, S. Daniels, S. Purkayastha, P. Juhasz, S. Martin, M. Bartlet-Jones, F. He, A. Jacobson, D.J. Pappin, Multiplexed Protein Quantitation in Saccharomyces cerevisiae Using Amine-reactive Isobaric Tagging Reagents*S, Molecular Cellular, Proteomics 3 (12) (2004) 1154–1169.
[26] H. Yu, Y. Liu, F. Yang, Y. Xie, Y. Guo, Y. Cheng, W. Yao, Synergistic efficacy of high-intensity ultrasound and chlorine dioxide combination for Staphylococcus aureus biofilm control, Food Control 122 (2021), 107822.
[27] Q. Shu, H. Lou, T. Wei, X. Zhang, Q. Chen, Synergistic antibacterial and antibiofilm effects of ultrasound and MEL-A against methicillin-resistant Staphylococcus aureus, Ultrasonics Sonochemistry 72 (2021), 105452.
[28] Y. Chen, L. Sheng, M. Gouda, M. Ma, Impact of ultrasound treatment on the foaming and physicochemical properties of egg white during cold storage, LWT 113 (2019), 108303.
[29] J. Dai, M. Bai, C. Li, H. Cui, L. Lin, Advances in the mechanism of different antibacterial strategies based on ultrasound technique for controlling bacterial contamination in food industry, Trends Food Sci. Technol. 105 (2020) 211–222.
[30] A. Sarjit, J.T. Ravensdale, R. Coorey, N. Fegan, G.A. Dykes, Salmonella response to physical interventions employed in red meat processing facilities, Food Control 103 (2019) 91–102.
[31] I.B. Holland, Rise and rise of the ABC transporter families, Res. Microbiol. 170 (2019) 304–320.
[32] P. Varmanen, J.L. Steele, A.M. Palva, Characterization of a prolinase gene and its product and an adjacent ABC transporter gene from Lactobacillus helveticus, Microbiology 142 (Pt 4) (1996) 809–816.
[33] J. Li, D. Liu, T. Ding, Transcriptomic analysis reveal differential gene expressions of Escherichia coli O157:H7 under ultrasonic stress, Ultrasonics Sonochemistry 71 (2021) 105418, https://doi.org/10.1016/j.ultsonch.2020.105418.
[34] K. Kobayashi, Gradual activation of the response regulator DegU controls serial expression of genes for flagellum formation and biofilm formation in Bacillus subtilis, Mol. Microbiol. 66 (2) (2007) 395–409.
[35] C.l. Fabret, J.A. Hoch, A Two-Component Signal Transduction System Essential for Growth of Bacillus subtilis: Implications for Anti-Infective Therapy, J. Bacteriol. 180 (1998) 6375–6383.
[36] X. Jin, J.E. Lee, C. Schaefer, X. Luo, A.J.M. Wollman, A.L. Payne-Dwyer, T. Tian, X. Zhang, X. Chen, Y. Li, T.C.B. McLeish, M.C. Leake, F. Bai, Membraneless organelles formed by liquid-liquid phase separation increase bacterial fitness, Sci. Adv. 7 (2021) eabh2929.
[37] A. Taha, E. Ahmed, A. Ismaiel, M. Ashokkumar, X. Xu, S. Pan, H. Hu, Ultrasonic emulsification: An overview on the preparation of different emulsifiers-stabilized emulsions, Trends Food Sci. Technol. 105 (2020) 363–377.
[38] B. Xu, J. Yuan, L. Wang, F. Lu, B. Wei, R.S.M. Azam, X. Ren, C. Zhou, H. Ma, B. Bhandari, Effect of multi-frequency power ultrasound (MFPU) treatment on enzyme hydrolysis of casein, Ultrasonics Sonochemistry 63 (2020), 104930.